Characterization of the Highest Slip Rate Fault in the Lake Tahoe Basin: Paleoseismic Investigation of the West Tahoe Fault

Proposal number
NEHRP External Grant Award Number: G11AP20129

Principal Investigator:
Gordon Seitz, PhD, CEG
Engineering Geologist

Seismic Hazard Assessment Program
California Geological Survey
345 Middlefield Road, MS 520
Menlo Park, CA 94025
650.688.6367

Gordon.Seitz@conservation.ca.gov

www.conservation.ca.gov/cgs

Introduction

The purpose of this report is to present results of the first trenching study of the West Tahoe fault (Seitz, 2015a, b, Seitz and Mareschal, 2014, Seitz, 2014), and put the results into the context of what is known about this fault's behavior. We used the most recent Lidar data (Watershed Sciences, 2010) to characterize the activity of the onshore portions of the West Tahoe fault (fig.1). Details of the onshore West Tahoe fault mapping have been further evaluated in Seitz (2015b, in review), and Kent et al. (2015).

South of Emerald Bay, the West Tahoe fault extends onshore as two parallel strands (fig. 2). In this area, the West Tahoe fault is expressed as a sharp fault scarp, several meters in height, primarily in glacial deposits of Tahoe and Tioga age. Kent et al., (2005) and Dingler et al., (2009) estimate the slip rate on the West Tahoe fault to be 0.6-1.0 mm per year, the highest of any fault in the Tahoe basin, based on displacement of a submerged and dated shoreline across the southern Tahoe basin.

The central portion and majority of the Tahoe basin is covered by Lake Tahoe. This report focuses on the West Tahoe fault where it emerges onshore at Emerald Bay to its southern terminus south of Highway 50 (fig. 2). This study used available highest resolution Lidar data (Watershed Sciences, 2010) to evaluate this portion of the West Tahoe fault. In order to capture a complete event record we selected a trench site where the fault is a single strand, south of Fallen Leaf Lake.

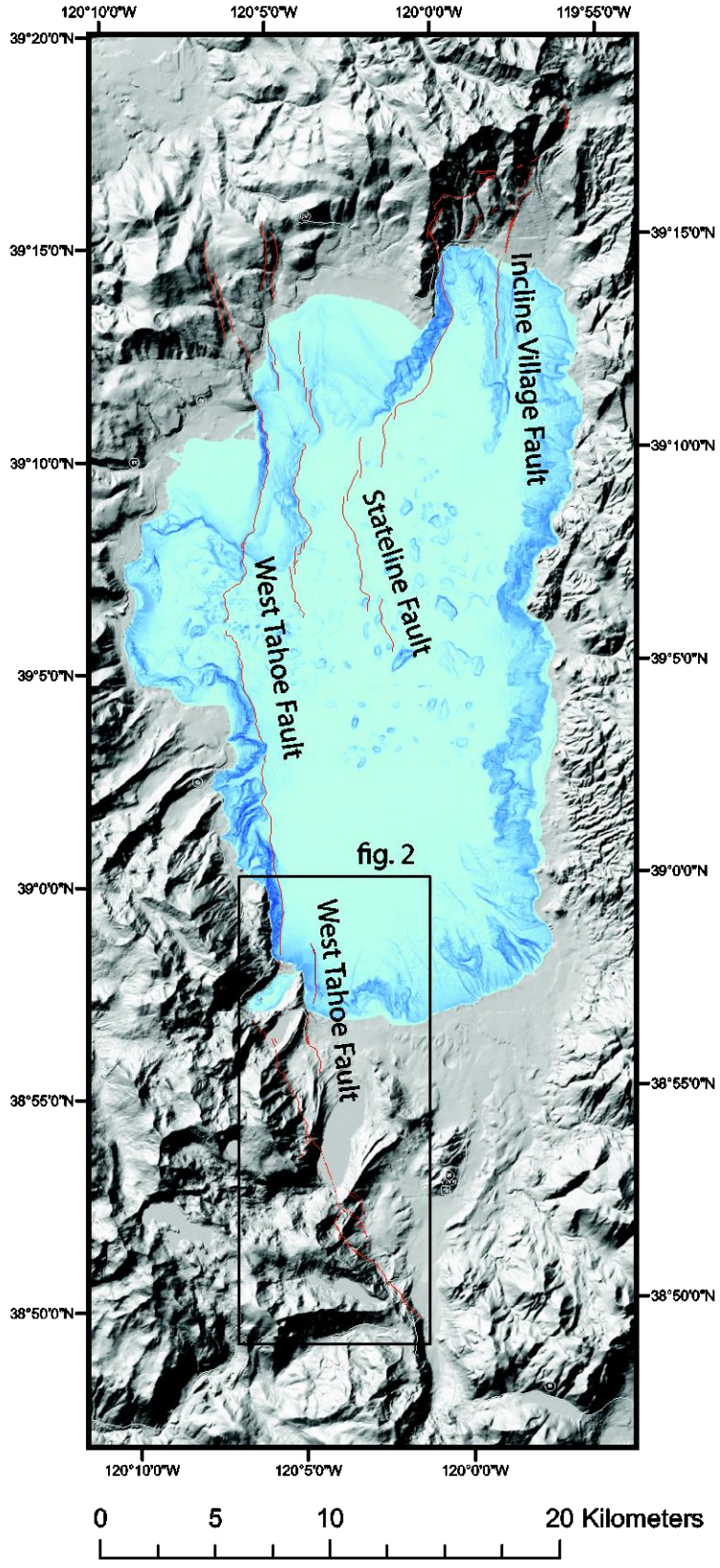

Figure 1. Tahoe Basin Fault Map. Active faults are shown with red lines. Three active faults cross the Tahoe basin: West Tahoe fault, the Stateline fault and the Incline Village fault. The focus of this report is on the southern portion of the West Tahoe fault where it extends onshore south of Emerald Bay. High resolution multibeam bathymetry and Lidar topography has been instrumental in revealing the exact locations of active faults. The onshore image is a hill shade, the offshore is a slope shade. The figure 2 extent is indicated.

Geologic Setting

The Tahoe Basin is bounded by the Sierra Nevada on the west and the Carson Range to the east. These ranges are predominately composed of Cretaceous-age granitic rocks mantled by Tertiary-age volcanic rocks (Saucedo, 2005). West of Fallen Leaf Lake, the granitic rocks surround older metamorphic roof pendants. The Tahoe basin is the westernmost basin of the Basin and Range extensional province. The basin is an asymmetric half graben (Dingler et al., 2009) and has been active for at least the past 3 m.y. (Surpless et al., 2002, Faulds et al., 2005).

The southwest portion of the Tahoe basin that includes the West Tahoe fault has a flatter shelf that extends from the lake to the highlands in the west (fig. 2). This shelf increases in width, from about 1 km north of Emerald Bay to 12 km at the trench site. In general, these flatter portions that abut the lake are underlain by glacial, fluvial, and lacustrine deposits. North of Emerald Bay, this bedrock shelf is elevated, which is consistent with its position on the uplifted footwall block of the offshore West Tahoe fault.

On and offshore studies in the Tahoe basin (Seitz and Kent, 2004, Kent et. al, 2005, Dingler et al., 2009, Brothers et al., 2009, Smith et al., 2013, Maloney et al, 2014, Kent et al, 2015), have revealed three active normal faults that are significant seismic sources (fig. 1). Using high-resolution seismic CHIRP (Compressed High Intensity Radar Pulse) profiles, combined with age dating of sediment cores using radiocarbon (C-14) and optically stimulated luminescence (OSL) techniques, have allowed estimates for slip rates. Offset submerged paleolake terraces and a catastrophic slide debris deposit provide markers for vertical slip rates of 0.6 mm/yr (0.44-1.1), 0.45 mm/yr (0.35-0.6) and 0.2 mm/yr (0.12-0.3) on the West Tahoe, Stateline and Incline Village faults, respectively (Kent et al., 2005; Dingler et al., 2009). Total extension across all three basin forming faults is estimated to be 0.84 mm/yr (0.53-1.15), or more than 30% of east-west extension observed along Sierra Frontal faults through geodetic measurements spanning the Walker Lane (Hammond and Thatcher, 2004, Bormann, 2013).

The West Tahoe fault is the range bounding, east-dipping normal fault along the west margin of the basin and has a mapped length of 45 km (fig. 1). It is largely located along the western base of Lake Tahoe at a water depth of 400-500 m and modelling has validated the significant tsunami and seiche hazard (Ichinose et al., 2000). In the lake, the fault has clearly defined scarps that offset submarine fans, lake-bottom sediments, and the McKinney Bay slide deposits (Hyne et al, 1972; Gardner et al, 2000; Kent et al, 2005; Dingler et al. 2009). Recent work analyzing sediment cores from the lake bottom has clearly shown that earthquakes on the local faults trigger landslides in the lake (Smith et al., 2013). These triggered landslides in turn stir up the lake sediments which form distinct and wide-spread turbidite deposits. Sediment cores have revealed a long-term record of strong earthquake ground shaking frequency, with between 14 to 17 events recognized in the past 12 thousand years.

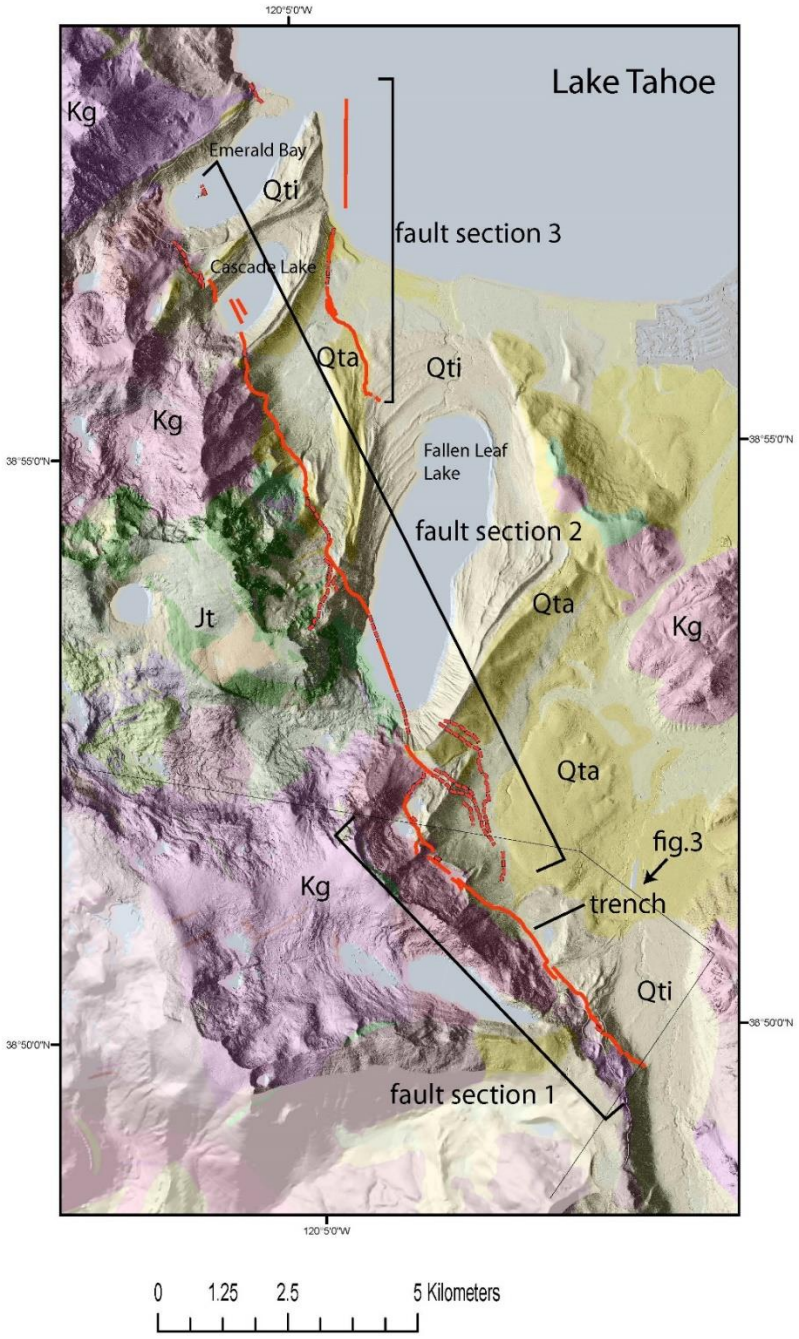

Figure 2. West Tahoe Fault Map. This map shows the southern portion of the West Tahoe fault where it extends onshore south of Emerald Bay. The fault has been divided into fault sections based on trend and continuity. From youngest to oldest general geological units are indicated:
Jt-Jurrasic Metamorphics, Kg-Cretaceous Granitics, Qta-Tahoe-age Glacial Deposits, Qti- Tioga-age Glacial Deposits. A fault investigation location with a trench is shown in fault section 1. This is the only onshore location where the faulted deposits are dated directly. A detailed geomorphic fault evaluation is presented in Seitz (2015b).

Other Interpretations of Active Faulting

Following the multibeam bathymetric survey of Gardner et al. (1998, 2000) several active faults were mapped in Lake Tahoe. Some of these faults were previously recognized as active by Hyne et al. (1972) in their offshore study. Schweickert et al. (1999, 2000b) incorporated the offshore faults into a basin-wide mapping effort that included onshore extensions of these faults, and many more features interpreted as active faults. This work was summarized in the "Preliminary map of Pleistocene to Holocene faults in the Lake Tahoe Basin, California and Nevada" (Schweickert et al., 2000b). This map, as stated in their disclaimer, was a preliminary generalized map that was not intended to be used for planning purposes addressing seismic hazards. In practice this caution was often ignored and the map was used for planning purposes. The detailed offshore studies based on seismic profiling and sediment cores (Kent et al., 2005, Dingler et al, 2009) have provided robust slip rate estimates. In contrast, the distribution and character of the onshore faults has been controversial (Bell et al., 2002, Kent et al., 2015, Dingler et al., 2009), and many features mapped as faults were later found to be non-tectonic geomorphic scarps or lineaments. In 2005, Saucedo published an updated geologic map of the Tahoe basin. This mapping effort included an evaluation of mapped onshore faults from the Schweickert et al., (2000b) map. Peer review, including group field reviews, of onshore faults north of Emerald Bay questioned the activity, and the existence of faults, some of which were subsequently not included in the map by Saucedo (2005). Dingler et al. (2009) could not find evidence of faults that Schweickert et al. (2000, 2004) named the "Tahoe Sierra Frontal Fault" in Emerald Bay. More recent mapping by Howle et al., (2012) using a Lidar survey by the Army Corps of Engineers has reintroduced the "Tahoe Sierra Frontal Fault" as a zone of active faulting. In general, availability of increasingly detailed and extensive Lidar surveys has increased our confidence in evaluating the geomorphology and origin of fault-like features. Further detailed evaluation of the faults mapped by Howle et al., (2012), used a more recent, Lidar survey by Watershed Sciences (2010). This survey was higher resolution, and more extensive than the 2008 USACE Lidar survey used by Howle. We have conducted a detailed fault evaluation for surface rupture hazard (Bryant, 2009) and have also not found any evidence to support active faulting of a "Tahoe Sierra Frontal Fault" (Seitz, 2015b).

Glacial Deposits and Geomorphology

Most of the area crossed by the on-land sections of the West Tahoe fault is underlain by glacial deposits of Pleistocene age. Two clearly recognized late Pleistocene-age glaciations are referred to as the Tahoe and Tioga (Blackwelder, 1931, Birkeland, 1961, 1964; McCaughey, 2003). In general, the two glacial maxima are recognized as the highest lateral moraines that extend from the margins of glacial valleys at the range front towards the shoreline (fig 5). The moraine crests are about 100 to 200 m higher than the surrounding landscape. The older Tahoe-age maximum moraines generally lie in a slightly higher landscape position than the younger Tioga-age moraines. The Tioga-age moraines parallel the Tahoe moraines, and often truncate the lower

portions of them. Thus, the entire set of Tioga moraines is generally much more complete. For example, at Fallen Leaf Lake a remarkable series of 22 Tioga-age recessional moraines is preserved (fig. 1, 2, and 5).

Most of the age estimates for glacial deposits in the Tahoe basin rely on correlations with numerically dated moraines elsewhere along the Sierra Nevada. These regional correlations are fraught with uncertainty and hence we focus here on several age determinations from the Tahoe basin that can be correlated directly to faulted deposits in the evaluated area.

On the west side of Lake Tahoe near Meeks Bay, north of Emerald Bay, the two highest moraine crests were dated using cosmogenic nuclide surface exposure analyses for ^{26}AL and ^{10}Be (Howle et al., 2005; 2012). The well-preserved moraines at Meeks Bay consist of granitic till. Several samples were taken from the tops of boulders. The highest Tahoe-age moraines were dated at 69.2±4.8 ka, and the Tioga-age moraine was dated at 20.8±1.4 ka. These dates are currently the only direct dates of these moraines in the Tahoe basin, and appear reasonable compared to other Sierra Nevada localities**.**

Relative dating of the highest moraines throughout the basin is possible because the two-fold glacial history has resulted in a relatively simple and distinct set of two moraine complexes of Tioga and Tahoe age. Even prior to the availability of high resolution topography, it was recognized that the older Tahoe-age moraines exhibited rounder, flatter, and wider crests with more deeply weathered boulders (Blackwelder, 1931, Birkeland, 1961, 1964, McCaughey, 2003). Specifically for the southwest Tahoe Basin, McCaughey (2003) quantified the different weathering related field parameters that differentiate the Tahoe and Tioga-age glacial deposits. McCaughey was able to show that the moraine crests flatten significantly over time, allowing the distinction between the Tahoe-age moraines at 70 ka and the Tioga-age moraines at 20 ka. This difference in moraine crest geomorphology can now be used as a relative dating method, using the dated Meeks Bay moraines as calibration (fig. 5).

Active Fault Geomorphology

West Tahoe Fault Sections

The West Tahoe fault is described as three sections that are continuous, without major steps or trend changes (fig.2). Specific details of this mapping are presented in a "Fault Evaluation Report" prepared for surface rupture hazard (Seitz, 2015b in review). Sections, 1, 2, and 3 are 6 km, 12.2 km, and 5.5 km long, respectively. These fault sections exhibit an overlapping right-stepping pattern, with a 0.5 km step east from section 1 to section 2, and a 1 km step from section 2 to section 3. The northern portion of section 3 trends offshore. North of Emerald Bay the uplifted shoreline is consistent with an offshore West Tahoe fault accommodating the entire slip budget of the fault. This stepping pattern continues offshore along the mouth of McKinney Bay where about 1 km further east the Stateline fault trends approximately parallel to the West Tahoe fault (fig. 1).

The extent of the Lidar survey used by Howle et al. (2012) does not include fault section 1 described in the below. Additionally, addressing general differences in onland and offshore fault mapping, Kent et al. (2015) conducted a basin-wide fault evaluation that used the Watershed Sciences (2010) Lidar survey and the most comprehensive collection of offshore high-resolution seismic profiles. Based on the highest-resolution 2010 Lidar data (Watershed Sciences) Seitz (2015b, in review) and Kent et al. (2015) did not find evidence of active faulting onshore north of Emerald Bay west of Lake Tahoe.

Fault Section 1

Fault section 1 is the southernmost fault strand extending from Christmas Valley to Angora Lakes (fig 2). At the southern end of the fault, the fault scarp does not extend across the flat valley floor, and several recessional moraines do not exhibit faulting. The linear valley margin, shown as a concealed fault by Saucedo (2005), is more likely due to glacial erosion.

To the north, the fault is located along the west side of the steep-sided glacial valley, alternating between the flat valley floor and glacial deposits. Because the glacial deposits may extend to considerable elevations above the valley, the fault climbs the valley slopes. The valleys have been dominantly shaped by glaciers and their deposits and the movement on the West Tahoe fault has resulted only in a slight reshaping since the Pleistocene glaciations. From its southern end in Christmas Valley, the fault scarp climbs up the side of the valley slope northward towards the trench site. The east-facing scarp along this stretch is well defined in the Lidar imagery with scarp heights on the order of 1-3 m in Tioga-age glacial deposits and overlying alluvium. Near Osgood Swamp (fig.3) the fault is well expressed with a ~3 m high scarp in Tioga-age till. Between the lateral moraines that surround the recessional moraine complex that includes Osgood Swamp, the east-facing fault scarp is less steep. In this area the fault scarp is less steep because the surface deposits include a thin layer of late Holocene sandy alluvium.

North of Osgood Swamp, a well-defined scarp in Tioga age till is continuous towards Angora Lakes (fig. 3). The northern end of the fault between the Angora Lakes curves to the east towards the southern Fallen Leaf right lateral moraines.

Fault section 1 to section 2 Step-Over

North of the Osgood Swamp moraine complex, the section 1 fault climbs up to Earthquake Lake (Kent et al., 2015) and continues to Angora Lakes. Here the fault takes a nearly right angle 500 m turn down slope, to the east, where the fault scarp nearly intersects the first prominent section 2 fault scarp, which cuts across the extension of the Tahoe/Tioga –age moraine crests (fig. 3,5). This fault bend matches the topography in that it runs along the base of the range front. Section 1 and section 2 fault sections overlap by 1.7 km and an additional parallel branch fault exists further east. Overall this type of fault structure has been described as a step-over or relay ramp structure with linkage (Faulds et al., 2011). All the faults in the step-over structure appear to have east-facing scarps. The western-most strands of this step-over have the sharpest scarps,

which suggest greater recent activity and that the most recent surface ruptures have been localized here, based on the continuity from the trench exposure at Osgood Swamp.

Fault Section 2

Section 2 extends from north of the Osgood Swamp moraines 12.5 km (fig. 2) to Emerald Bay. Where Section 2 branches from Section 1, it can be traced as a series of east-facing scarps that extend more northerly than Section 1**.** Section 2 consists of sharp scarps in mostly Tioga-age glacial deposits. Within a notch with a flat valley trending northwest to southeast across the Tahoe and Tioga-age right lateral moraines has a clear down to the east scarp along the west side of this notch. A sharp east-facing scarp in Tioga glacial till exists within a flat-valley notch that cuts across the upper Fallen Leaf Lake right-lateral moraines. The origin of this notch appears to be fluvial during or post the Tioga-age glacial period. There is no evidence for a west-dipping antithetic fault on the east side of this notch. The east-facing fault scarp is 3.8 m high (this study measured with the 2010 Lidar survey, and 2008 Lidar survey used by Howle et al., 2012) and is beveled. This is indicative of multiple events, most likely three, based on comparisons the trench exposure at Osgood Swamp (Seitz, 2015, a, b, Seitz and Mareschal, 2013) and similar scarps at the northern end of Section 1 at Angora Lakes (Kent et al., 2015).

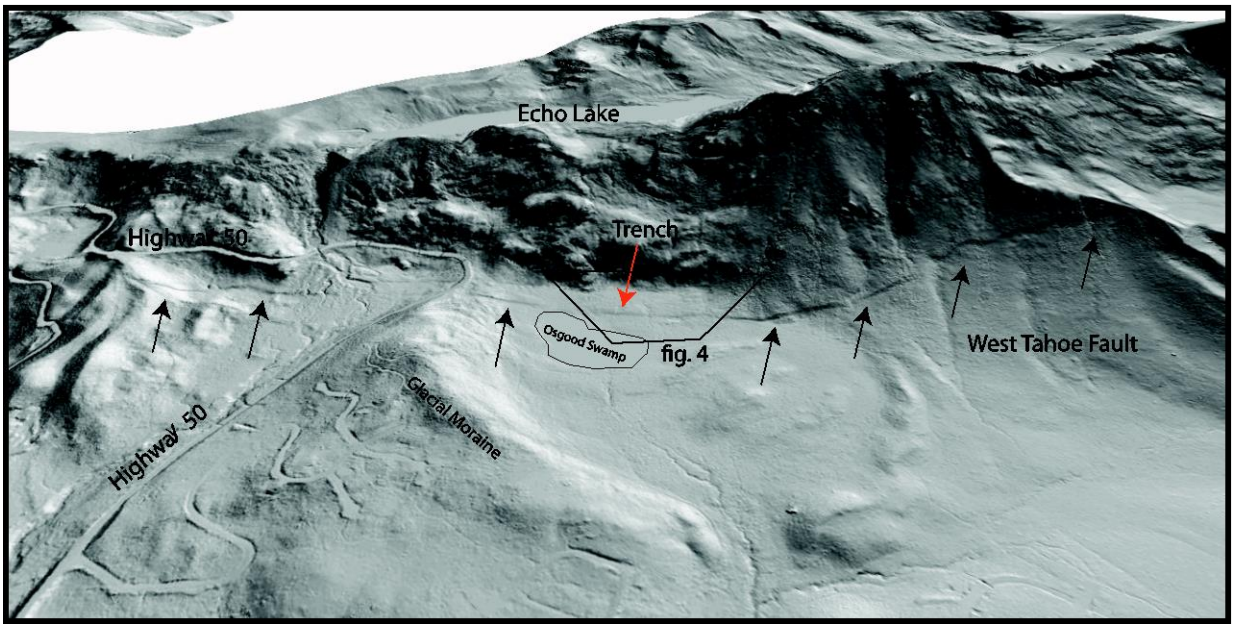

Figure 3. Oblique Lidar Hill shade. The West Tahoe fault is expressed as a sharp continuous scarp indicated by black arrows. The trench location is shown with a red arrow. The trench site is located within a recessional moraine complex. The glacier flowed from the Echo Lake basin, and the U-shaped notch directly west of the site is evident.

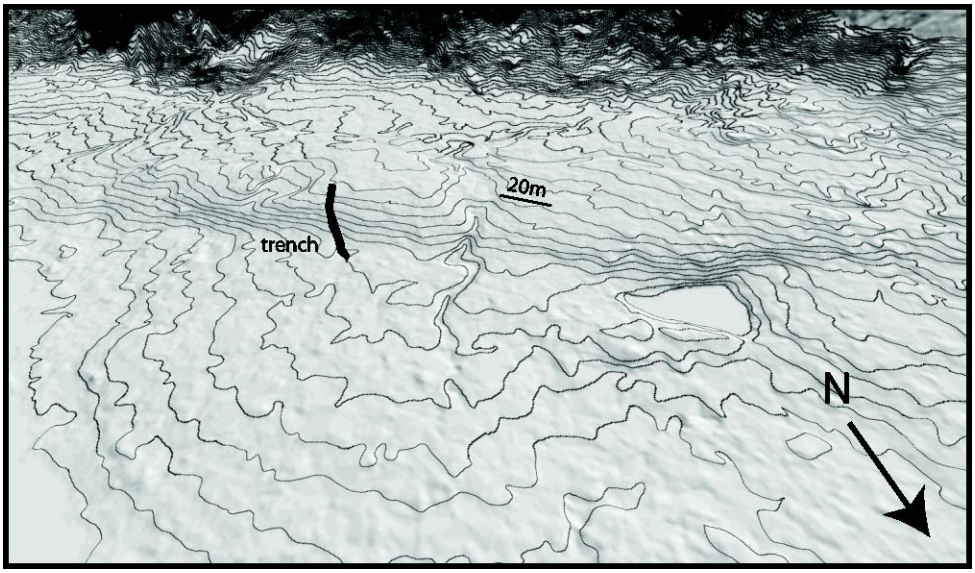

Figure 4 Oblique Contoured Hillshade. This image is based on a 0.5 m Lidar derived bare earth Digital Elevation Model. The contours are 0.5 m. The 3 meter high fault scarp is well expressed in the Tioga-age landscape covered by a thin veneer of late Holocene alluvium. Note the channel incised into the scarp near the scale bar. This scarp derived channel forms the apex of an alluvial fan which only occurs on the downthrown fault block. These fan deposits are cut by the latest event providing additional evidence of multiple earthquakes.

The east facing scarp in Tioga age deposits can be traced north to the crest of the right- lateral moraine south of Fallen Leaf Lake. The north side of this moraine along the projection of the fault has been modified by numerous debris slide and debris flow scars, removing any fault related features. Within Fallen Leaf Lake, the fault has been clearly observed in seismic profiles and multibeam bathymetry (Brothers et al., 2009, Maloney et al., 2013). Within the array of extensive seismic profiles, the fault is expressed as a single strand with down to the east displacement. Maintaining its trend, the fault emerges on the northwest side of Fallen Leaf Lake with a clear scarp expressed as a steepened slope on the lake side of the moraine. From the Fallen Leaf Lake left-lateral moraine crest, the fault scarp is clearly expressed to Cascade Lake. Along the range front, glacial deposits are buttressed relatively high, this leads the fault to daylight similarly high along the slope, following a similar pattern as observed along section 1.

In Cascade Lake two fault strands are observed in seismic profiles (Maloney et al., 2014) slightly to the east of the onshore projection. Geomorphically, the fault is much less well expressed on the north side of Cascade Lake over the moraine crest towards Emerald Bay.

Fault Section 3

Section 3 is comprised of a parallel strand 1.5 km east of fault Section 2, 0.7 km northwest of the northwest end of Fallen Leaf Lake (fig 2, 5). This fault scarp has an onshore extent of 2.8 km,

and may extend over 5 km offshore. It overlaps with Section 2 a minimum of 2.8 km and a maximum of 4.5 km. Onshore, the fault consists of a well-defined scarp in Tioga and Tahoe-age glacial deposits. A remarkable series of recessional moraines is preserved along the north side of Fallen Leaf Lake (fig. 5). These recessional moraine crests range in age from the outermost at with a Tioga maximum age of about 20 ka (Howle, et al., 2005, 2012), to about 10-12 ka, in Fallen Leaf Lake (Seitz and Mareschal, 2014, Seitz, 2015b). A series of these youngest moraines adjacent to Fallen Leaf Lake are not cut by this fault, and no fault was recognized in the high resolution seismic CHIRP profiles along this trend in Fallen Leaf Lake to the south (Kent et al., 2015, Brothers et al., 2009, Maloney et al., 2013). Scarp heights along this fault are about 3 m in Tioga-age deposits, increasing to about 10 m in Tahoe age deposits where the fault extends offshore adjacent to the left-lateral Cascade Lake moraine. Dingler et al. (2009) describes an offshore side slope bench with pock marks that was interpreted as the possible existence of an active fault roughly along trend with this fault offshore to the north. This fault strand may represent a likely connecting structure to the most active portion of the West Tahoe fault which lies offshore along the western base of Lake Tahoe.

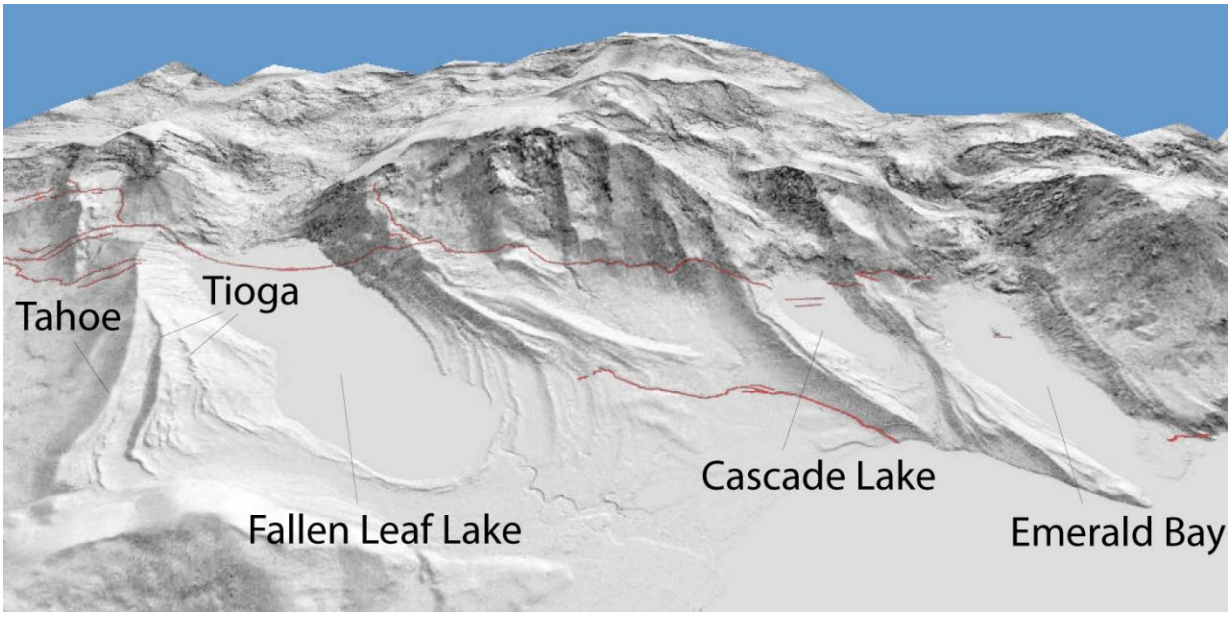

Figure 5. Glacial Moraines along the west shore of Lake Tahoe. The paired glacial moraines which extend the highland glacial valleys from the range front towards the Lake Tahoe, but also formed Fallen Leaf Lake , Cascade Lake and Emerald Bay. The older flatter crested Tahoe-age (70 ka) moraine along Fallen Leaf Lake and a sharper crested Tioga-age (20 ka) maximum moraine are shown. The West Tahoe fault is shown with red lines.

Subsurface Investigation

In October 2013 we conducted the first trenching study of the West Tahoe fault (fig. 2, 3, 4) ~3.5 km from the southern end of the mapped fault, adjacent to Osgood Swamp (Seitz, 2015a, b, Seitz

and Mareschal, 2014, Seitz, 2014). The trench site is located within a moraine complex between prominent lateral moraines and upslope of a series of Tioga-age recessional moraines. The glacier originated from the Echo Lake valley to the west and flowed over the range crest eroding a prominent U-shaped notch in the ridge before flowing down 300 m to the flat valley floor. A site with fine-grained surface sediments was selected, as opposed to the boulder-rich moraine sediments that cover most of the onshore fault. At the trench site a 1.5 m surface layer of post-glacial sandy alluvium has resulted in a less steep scarp.

The excavation revealed an east-dipping, normal fault juxtaposing glacial deposits against datable peat-bearing and charcoal-rich younger alluvial sediments (fig. 6). The glacial deposits and peat layers were matched across the fault. Clear evidence for three earthquakes is based on scarp-derived colluvium, fissures, faulted scarp-related alluvium, liquefaction, and upward terminations of faults. Retro deformation of the faulted sediments results in co-seismic vertical displacements estimates of 1.4 m, 0.8 m and 1 m from the most recent to oldest event, respectively. Results from multiple C-14 analyses place the most recent event at ~5.5 ka, the penultimate event at ~7.2 ka, and the oldest event at ~9 ka (fig. 9). These events (Seitz, 2015a, b, Seitz and Mareschal, 2014) appear to correlate with offshore Lake Tahoe turbidites (Smith et al., 2013), and landslides in Fallen Leaf Lake (Maloney et al., 2013).

Event Evidence

The event evidence is described from the oldest to the youngest as shown schematically in fig. 9, based on the more complete south wall exposure.

Event 3

When post glacial peat unit 20 was the surface layer a vertical displacement of about 1 m occurred on the western primary fault strands, on fig.7 these strands are below the 10.2 ka date. After the event a scarp derived colluvial wedge formed, orange unit labeled Ev 3. A peaty soil unit 10 formed on the hanging wall block capping the colluvial wedge labeled Ev3.

Event 2

A 0.8 m vertical displacement occurs on the eastern primary fault strand, about 3 m to the east of the event 3 faulting. A scarp derived colluvial wedge unit 8, labeled Ev2 is deposited overlying unit 9 with 9.0 ka and 7.3 ka dates.

Event 1

A 1.4 m vertical displacement occurs, the penultimate colluvial wedge unit 8 is, and a scarp derived colluvial wedge unit 7 forms. The faulting is concentrated on the same eastern fault strand as in the penultimate event.

Chronology

The chronological software program Oxcal (Bronk Ramsey, 2009) was used to model the event ages. This program incorporates the C-14 dendro calibration with stratigraphic ordering constraints, and calculates posterior probability density functions for the event ages. The input consisted of 12 AMS C-14 dates that we pretreated at the LLNL/CAMS facility. All samples above Ev-3 (fig.10) consisted of detrital charcoal. Additional confidence in correlating units across the fault zone was gained by dating the peat unit 20 on the foot, hanging wall, and central blocks. Peat samples have the advantage over detrital charcoal because the samples consist of in situ carbon as opposed to detrital charcoal that can have considerable context uncertainty. Stratigraphic order is based on the units from which they were sampled. The model and event ages are presented in fig. 10.

Summary

The observed 3 m high geomorphic scarp is largely consistent with the 3.2 m of vertical stratigraphic displacement of unit 30. Some uncertainty in these vertical displacements is due to the limited exposure of unit 30 on the hanging wall fault block. Minor complications are attributed to ongoing and variable alluvial deposition on the footwall and hanging wall fault blocks. The event ages and vertical displacements are: Event 1: 5.5 ka, 1.4 m, Event 2: 7.2 ka 0.8 m, Event 3: 9.0 ka., 1.0 m. A closed interval slip rate estimate between event 3 and 1 results in a vertical slip rate of 0.62 mm/yr, which is consistent with the longer term rates determined offshore (Kent et al., 2005, Dingler et al., 2009). The longer than average open interval of 5.5 ka may suggest a higher strain release in a future earthquake. The relatively small fault steps between fault sections (fig.2) make it difficult to rule out a future full-mapped fault length rupture of 45 km. Given the vertical event displacements, scarp heights, and fault geometry, earthquakes in the plus M7 range are clearly possible. Further refinements in the chronology, paleoseismic reconstructions and correlations to other sites will be incorporated into the peer reviewed article in preparation.

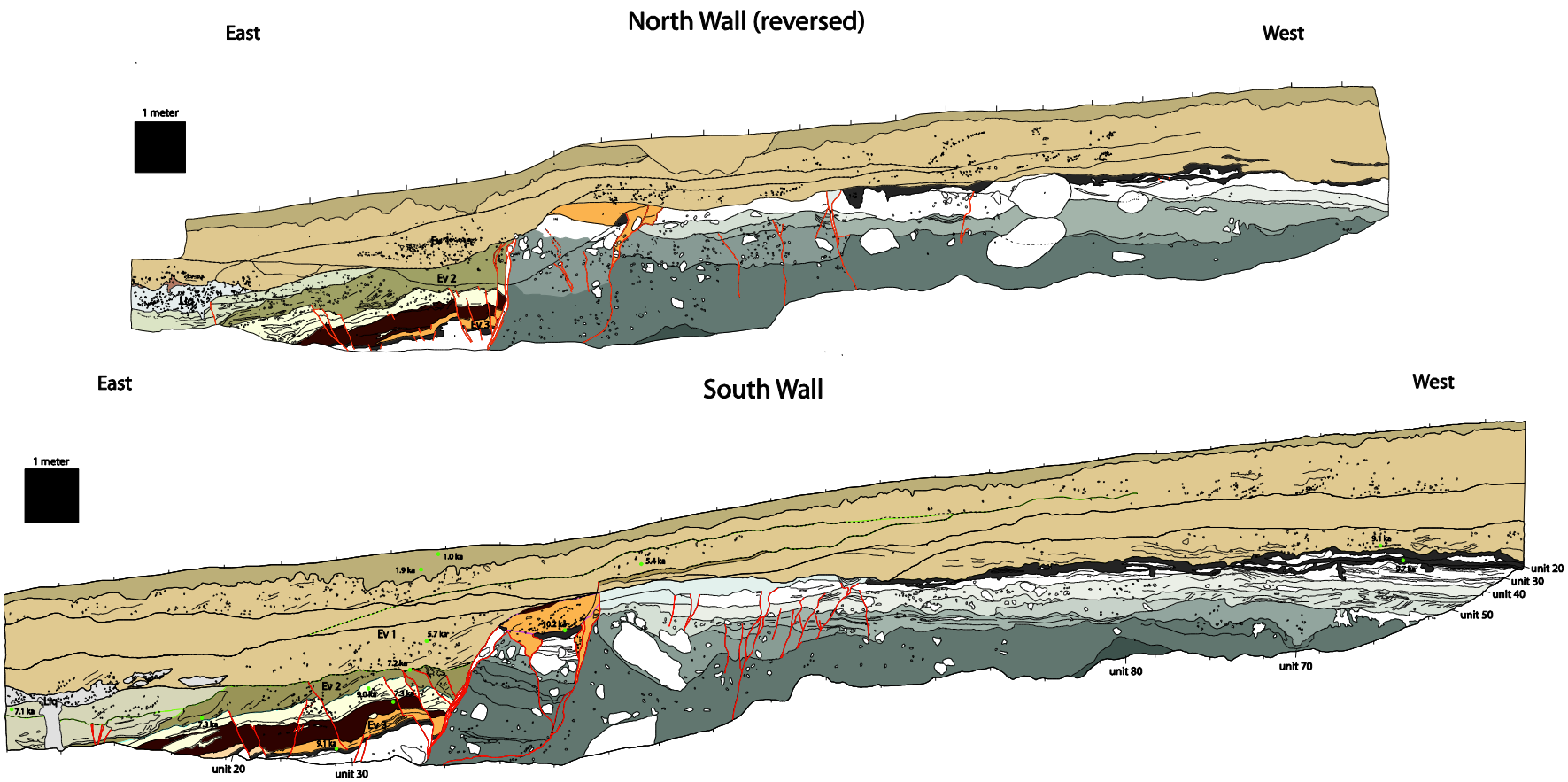

Figure 6 Trench Logs. Clear evidence for three earthquakes was identified during this 2013 USGS NEHRP funded project conducted by the California Geologic Survey (Seitz, 2015a,b, Seitz and Mareschal, 2014). Radiocarbon dating confirms three events in the past 10 ka. The main fault is the sharp left sloping contact between gray glacial sediments and brown alluvial and scarp derived colluvial sediments. The trench exposure is about 4 meters deep, image tiles are1 meter horizontal by 0.5 meter vertical. The excavation was benched, the upper bench is the separate top mosaic and log. The top contact is the original ground surface. The surface soils and colluvium thicken on the left down-faulted block. Fault trench location is indicated in fig. 2, 3, and 4.

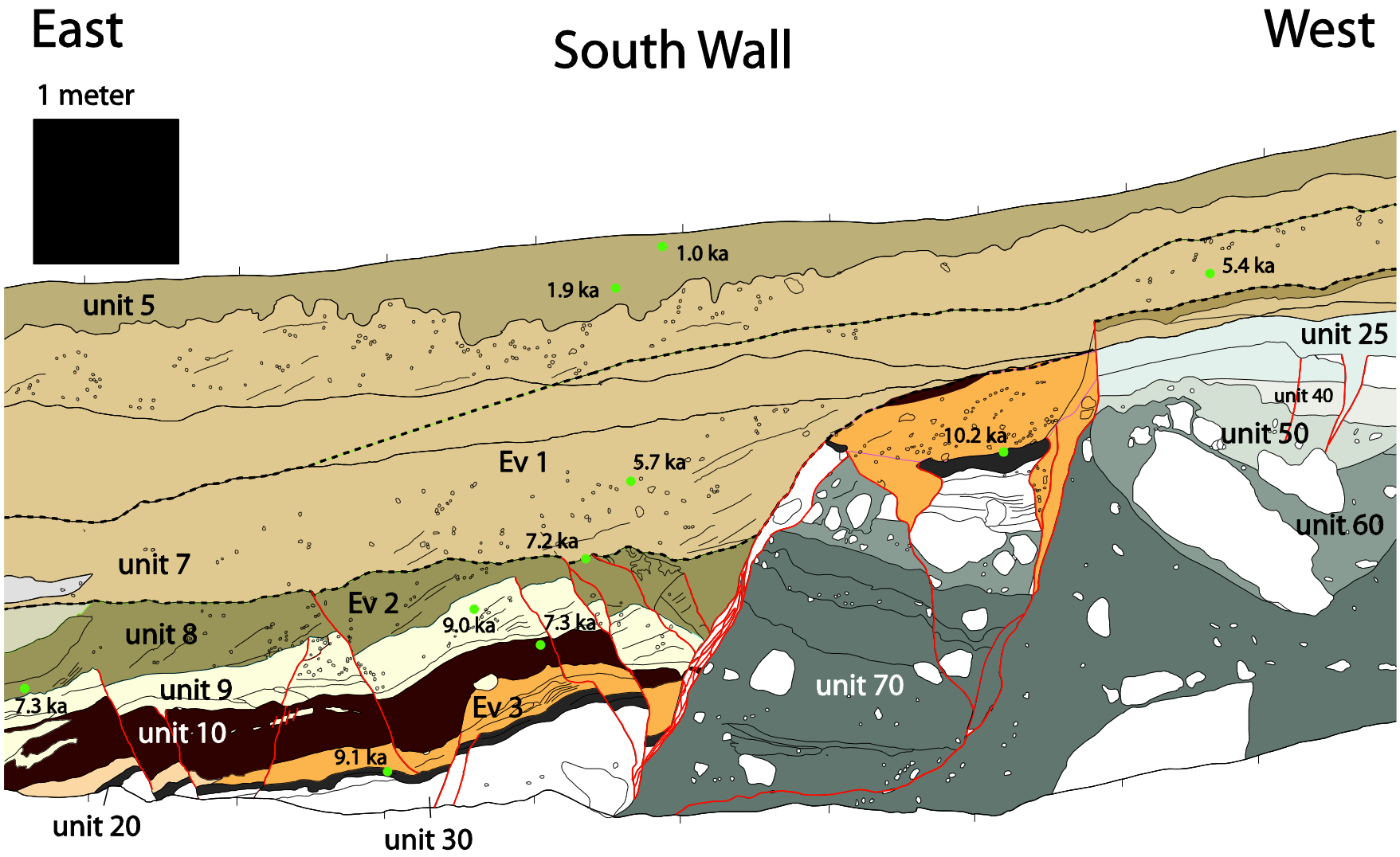

Figure 7. Trench Log Detail. Clear evidence for three earthquakes was identified during this 2013 USGS NEHRP funded project conducted by the California Geologic Survey (Seitz, 2015, Seitz and Mareschal, 2014). Radiocarbon dating confirms three events in the past 10 ka. Shown are best age estimates, the full age uncertainties are given in fig. 10. The main fault is the sharp east-dipping contact between gray glacial sediments and brown alluvial and scarp derived colluvial sediments. The trench exposure is about 4 meters deep, image tiles are 1 meter horizontal by 0.5 meter vertical. The excavation was benched, the upper bench is the separate top mosaic and log. The top contact is the original ground surface. The surface soils and colluvium thicken on the left down-faulted block. Fault trench location is indicated in fig. 2, 3 and 4.

Figure 8. Trench Photo Mosaic South Wall. The trench log on fig. 7 is based on this exposure, provided as a image mosaic here. This image shows the distinct stratigraphy. The main fault is the sharp east-dipping contact between gray glacial sediments and brown alluvial and scarp derived colluvial sediments. The trench exposure is about 4 meters deep, image tiles are 1 meter horizontal by 0.5 meter vertical. The excavation was benched, the upper bench is the separate top mosaic and log. The top contact is the original ground surface. The surface soils and colluvium thicken on the left down-faulted block. Fault trench location is indicated in fig. 2, 3 and 4.

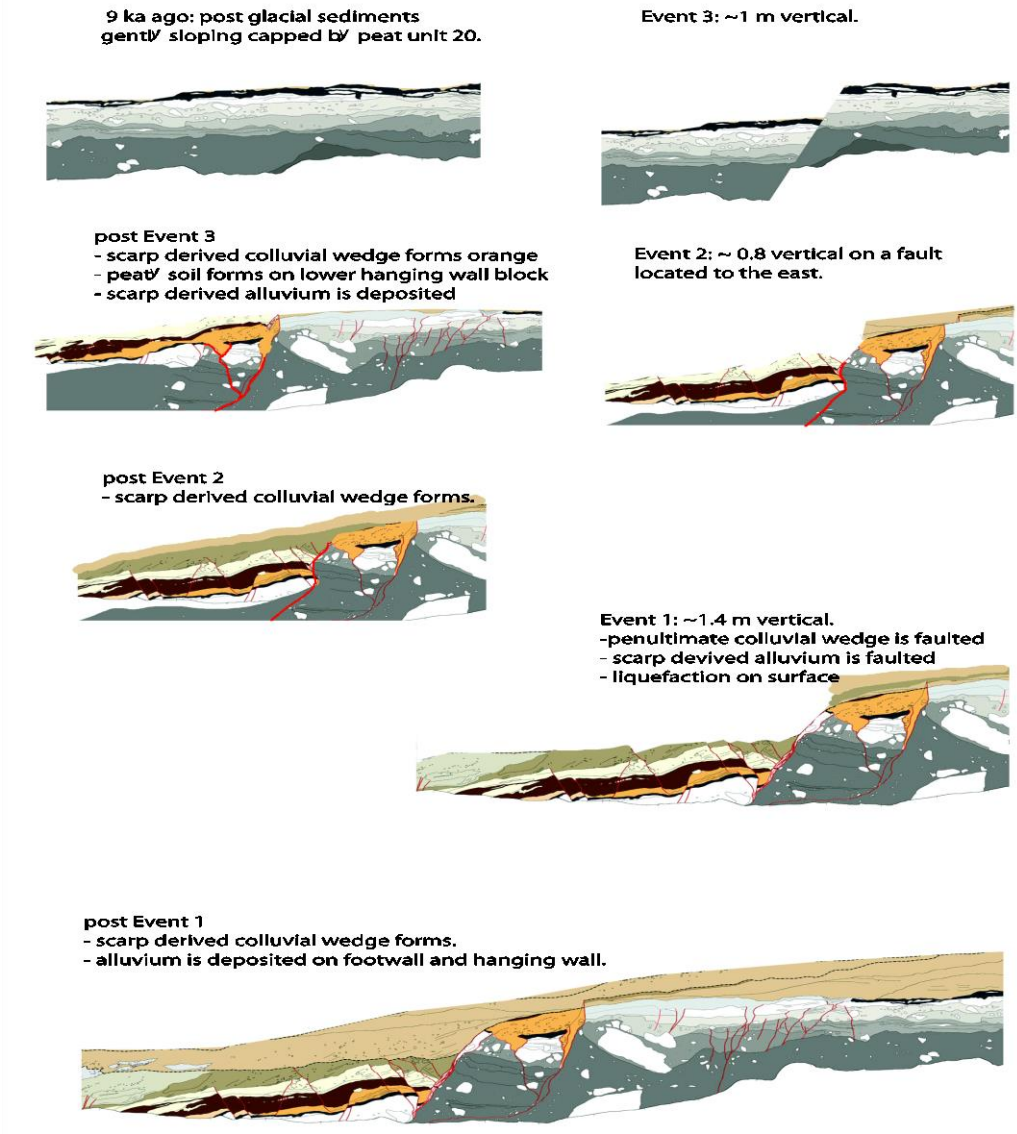

Figure 9 Schematic Event Retrodeformation. From the oldest to the most recent event this model shows how each event left a clear stratigraphic signature, which was interpreted to be the result of 3 vertical displacements.

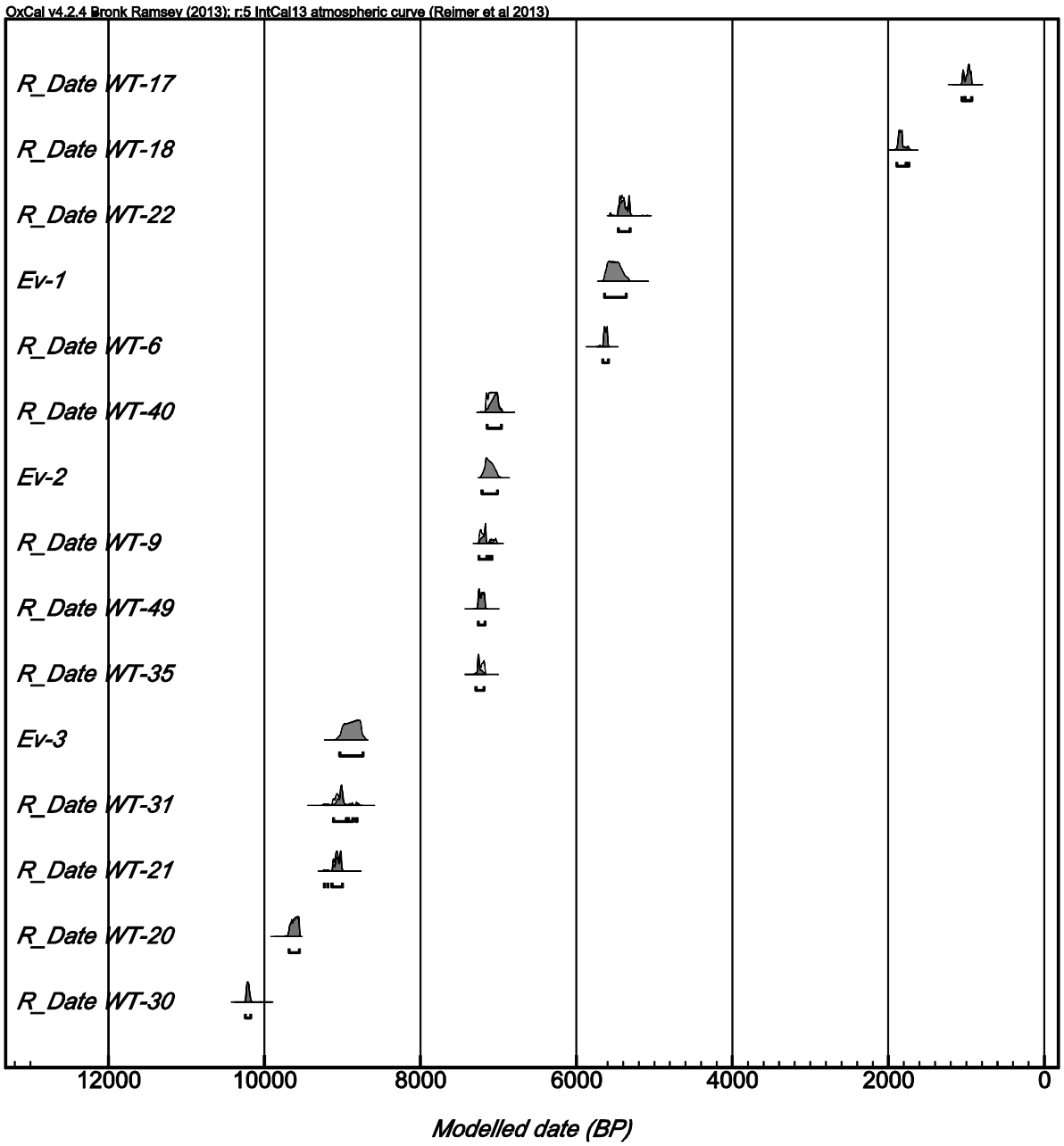

Figure 10 Chronological Event Model. The model is based on 12 AMS C-14 dates, 4 of which below Ev-3 consist of peat samples, the remaining samples consist of detrital charcoal. An ordering constraint was imposed. The event ages were calculated as lying between the overlying and underlying age ranges. The event ages are: Event 1: 5.5 ka, Event 2: 7.2 ka, Event 3: 9.0 ka. Oxcal v4.2.2 (Bronk Ramsey, 2009) was used.

NON-TECHNICAL SUMMARY

The West Tahoe fault is the primary active fault in the Tahoe basin. This study used a trench across the fault to examine and sample sediments deformed by earthquakes. This is the first onland record of past earthquakes of the West Tahoe fault. The event ages and vertical displacements are: Event 1: 5.5 ka, 1.4 m, Event 2: 7.2 ka 0.8 m, Event 3: 9.0 ka., 1.0 m (ka=1000 years before present). These results will be used to refine earthquake probability forecasts for the region.

REVIEW

Recognizing the subjective nature of paleoseismic trench observations, we made a concerted effort to have a meaningful field review in addition to the usual trench group showings. For the field review we contacted several expert paleoseismologists who spent considerable time in the trench, full days and several visits. The internal CGS reviewers were Tim Dawson, Ron Rubin, Tim McCrink, Pete Holland, and Anne Rosinski. Other reviewers with significant expertise included David Schwartz, Suzanne Hecker, USGS; Alan Ramelli, NBMG; Tom Sawyer, Piedmont Geoscience; Graham Kent, Steve Wesnousky, Jayne Bormann, UNR; Kelvin Berryman, GNS.

ACKNOWLEDGEMENT

This research was funded by the USGS NEHRP program. We thank our colleagues listed in the review section above for their efforts, and providing insights. We thank the USFS for granting us access to the site and in particular for assisting in the restoration.

REFERENCES

Bell, J.W., Ramelli, A.R., Caskey, J.S., 2002, Uncertainties associated with active faults mapped in the Lake Tahoe Basin, AEG annual meeting in Reno, abst.

Birkeland, P.W., 1961, Pleistocene history of the Truckee area, north of Lake Tahoe, California: Stanford University, Ph.D. dissertation, 126 p., plate 1, scale 1:62,500.

Birkeland, P.W., 1964, Pleistocene glaciation of the northern Sierra Nevada north of Lake Tahoe, California: Journal of Geology, v. 72, p. 810-825.

Blackwelder, E., 1931, Pleistocene glaciation in the Sierra Nevada and Basin Ranges: Geol. Soc. Amer. Bul, v.42, p 865-922.

Bormann, J. M., 2013, New Insights into Strain Accumulation and Release in the Central and Northern Walker Lane, Pacific-North American Plate Boundary, California and Nevada, USA [Doctorate Dissertation]: University of Nevada, Reno, 150 p.

Bronk Ramsey, C., 2009, Baysian analysis of radiocarbon dates, Radiocarbon, 51 (1), 337-360.

Brothers, D. S., Kent, G. M., Driscoll, N. W., Smith, S. B., Karlin, R., Dingler, J. A., Harding, A. J., Seitz, G. G., and Babcock, J. M., 2009, New constraints on deformation, slip rate, and timing of the most recent earthquake on the West Tahoe-Dollar Point Fault, Lake Tahoe Basin, California: Bulletin of the Seismological Society of America, v. 99, no. 2A, p. 499-519.

Bryant, W.A., and Hart, E.W., 2007, Fault-rupture hazard zones in California: California Geological Survey Special Publication 42, p.42.

Burnett, J.L., 1982, Geologic map of Lake Tahoe: California Division of Mines and Geology, unpublished mapping, scale 1:62,500.

Dingler, J., Kent, G., Driscoll, N., Babcock, J., Harding, A., Seitz, G., Karlin, B., and Goldman, C., 2009, A high-resolution seismic CHIRP investigation of active normal faulting across Lake Tahoe basin, California-Nevada: Geological Society of America Bulletin, v. 121, no. 7-8, p. 1089-1107.

Faulds, J.E., Henry, C.D., and Hinz, N.H., 2005, Kinematics of the northern Walker Lane: An incipient transform fault along the Pacific-North American plate boundary, Geology v. 33, p. 505-508.

Faulds, J.E., Hinz, N.H., Coolbaugh, M.F., Cashman, P.H., Kratt, C., Dering, G., Edwards, J. , Mayhew, B., McLachlan, H.. 2011. Assessment of Favorable Structural Settings of Geothermal Systems in the Great Basin, Western USA, In: Transactions. GRC Annual

Meeting; 2011/10/23; San Diego, CA. Davis, CA: Geothermal Resources Council; p. 777–783

Gardner, J.V., Mayer, L.A. and Hughes-Clarke, J.E., 1998, The bathymetry of Lake Tahoe, California-Nevada: U.S. Geological Survey Open-File Report OF 98-509.

Gardner, J.V., Mayer, L.A. and Hughes-Clarke, J.E., 2000, Morphology and processes in Lake Tahoe (California-Nevada): Geological Society of America Bulletin, v. 112, n. 5, p. 736-746.

Hammond, W.C., and Thatcher, W., 2004, Contemporary tectonic deformation of the Basin and Range Province, western United States; 10 years of observation with the Global Positioning System: Journal of Geophysical Research, v. 109, no. B8, doi:10.1029/2003JB002746.

Howle, J.F., Finkel, R.C., Seitz, G., 2005, Cosmogenic exposure ages for Tioga and Tahoe age moraines at Meeks Bay, Lake Tahoe, California, Geol. Soc. Amer. Annual mtg. abst.

Howle, J. F., G. W. Bawden, R. A. Schweickert, R. C. Finkel, L. E. Hunter, R. S. Rose and B. von Twistern, 2012, Airborne LiDAR analysis and geochronology of faulted glacial moraines in the Tahoe Sierra frontal fault zone reveal substantial seismic hazards in the Lake Tahoe region, California-Nevada, USA, Bull. Geol. Soc. Am., doi. 10.1130/830598.1

Hyne, N. J., Chelminski, P., Court, J. E., Gorsline, D. S., and Goldman, C. R., 1972, Quaternary History of Lake Tahoe, California-Nevada: Geological Society of America Bulletin, v. 83, no. 5, p. 1435-1448.

Ichinose, G.A., Anderson, J.G., Satake, Kenji, Schweickert, R.A. and Lahren, M.M., 2000, The potential hazard from tsunami and seiche waves generated by large earthquakes within Lake Tahoe, California-Nevada: Geophysical Research Letters, v. 27, no. 8, p. 1203-1206.

Karlin, R.E., Schweickert, R., Lahren, M., Shane, S., Patterson, M., Dinkelman, I. and Seitz, G., 2001, Late Quaternary history of landsliding and faulting in Lake Tahoe: Geological Society of America Abstracts with Programs, v. 33 n. 3, p. 71.

Kent, G. M., Babcock, J. M., Driscoll, N. W., Harding, A. J., Dingler, J. A., Seitz, G. G., Gardner, J.V., Mayer, L. A., Goldman, C. R., Heyvaert, A. C., Richards, R. C., Karlin, R., Morgan, C.W., Gayes, P.T., and Owen, L.A., 2005, 60 k.y. record of extension across the western boundary of the Basin and Range province: Estimate of slip rates from offset

shoreline terraces and a catastrophic slide beneath Lake Tahoe: Geology, v. 33, no. 5, p. 365-368.

Kent, G, Schmauder, G, Maloney, J., Driscoll, N., Kell, A.M., Smith, K., Baskin, R., Seitz, G., 2015, Reevaluating late Pleistocene and Holocene active faults in the Tahoe Basin, California-Nevada, AEG special pub.

Loomis, A.A., 1983, Geology of the Fallen Leaf Lake 15' quadrangle, El Dorado County, California: California Division of Mines and Geology Map Sheet 32, scale 1:62,500.

Maloney, J.M., Noble, P.J., Driscoll, N.W., Kent G.M., Smith, S.B., Schmauder, G.C., Babcock, J.M., Baskin, R.L., Karlin, R., Kell, A.M., Seitz, G.G., Kleppe, J.A., 2013, Paleoseismic history of the Fallen Leaf Segment of the West Tahoe-Dollar Point fault reconstructed from slide deposits in the Lake Tahoe Basin, California-Nevada, Geosphere, v. 9, no. 4, p. 1065-1090. doi: 10.1130/GES00877.1.

McCaughey, J.W., 2003, Pleistocene glaciation of the southwest Tahoe Basin, Sierra Nevada, California: University of Nevada, Reno, M.S. thesis, 179 p., plate 1, scale 1:15,400.

Saucedo, G. J., 2005, Geologic map of the Lake Tahoe Basin, California and Nevada: California Geological Survey, Regional Geologic Map No. 4, scale 1:100,000.

Schweickert, R. A., Lahren, M. M., Smith, K., and Karlin, R., 1999, Preliminary fault map of the Lake Tahoe basin, California and Nevada: Seis. Res. Lett., v. 70, p. 306-312.

Schweickert, R.A., Lahren, M.M., Karlin, R.E., Smith, K.D. and Howle, J.F., 2000b, Preliminary map of Pleistocene to Holocene faults in the Lake Tahoe Basin, California and Nevada: Nevada Bureau of Mines and Geology Open-File Report 2000-4, scale 1:100,000

Schweickert, R.A., Lahren, M.M., Karlin, R., Howle, J. and Smith, K., 2000a, Lake Tahoe active faults, landslides, and tsunamis, in Lageson, D.R., Peters, S.G. and Lahren, M.M., editors, Great Basin and Sierra Nevada: Geological Society of America Field Guide2, p. 1-22.

Schweickert, R. A., Lahren, M. M., Smith, K. D., Howle, J. F., and Ichinose, G. A., 2004, Transtensional deformation in the Lake Tahoe region, California and Nevada, USA: Tectonophysics, v. 392, no. 1-4, p. 303-323.

Seitz, G., and Kent, G, 2004, Closing the Gap between On and Offshore Paleoseismic Records in the Lake Tahoe Basin, NEHRP external tech report, 04HQGR007

Seitz, G. and Mareschal, M., 2014, Multiple-Event Deformation on the West Tahoe Fault from Lidar and Trenching: Reconciling On and Offshore Paleoseismology, American Geophysical Union, Fall Meeting 2014, abstract #T41C-4666

Seitz, G. 2015a, Tahoe Basin Fault Behavior from Integration of On and Offshore Paleoseismology, Basin and Range Province Seismic Hazards Summit III, Salt Lake City, Utah Geological Survey publications, p.1-4.

Seitz, G. 2015b in review, West Tahoe Fault Evaluation Report 261, California Geological Survey, p.1-28.

Seitz, G.G., 2014, Seismic Hazard Investigation of Lake Tahoe Using New Remote Operated Submarine: Dive Test in Support of Antarctic Subglacial Research (WISSARD) Project, Alfred E. Alquist Seismic Safety Commission, California Seismic Safety Commission publication.

Smith, S.B., Karlin, R.E., Kent, G., Seitz, G., and Driscoll, N.W., 2013, Holocene subaqueous paleoseismology of Lake Tahoe: Geological Society of America Bulletin, v. 125, p. 691–708, doi:10.1130/B30629.1.

Surpless, B.E., Stockli, D.F., Dumitru, T.A., and Miller, E.L., 2002, Two –phase westward encroachment of Basin and Range extension into the northern Sierra Nevada, Tectonics v.21, 1002.

Unruh, J., Humphrey, J., and Barron, A., 2003, Transtensional model for the Sierra Nevada frontal fault system, eastern California: Geology, v. 31, no. 4, p. 327-330.

Wells, D., and Coppersmith, K.J., 1994, New empirical relationships among magnitude, rupture length, rupture width, rupture area, and surface displacement: Bul. Seis. Amer., v.84, p. 974-1002.

Watershed Sciences, 2010, LiDAR Remote Sensing, Lake Tahoe Watershed, prepared for the Tahoe Regional Planning Agency, January 31, 2011.